How to cite: *Angew. Chem. Int. Ed.* **2024**, *63*, e202315872
doi.org/10.1002/anie.202315872

Asymmetric Hydrogenation

Unlocking the Asymmetric Hydrogenation of Tetrasubstituted Acyclic Enones

Jorge Faiges, Maria Biosca, Miquel A. Pericàs, Maria Besora, Oscar Pàmies, and Montserrat Diéguez**

Dedicated to Professor Andreas Pfaltz

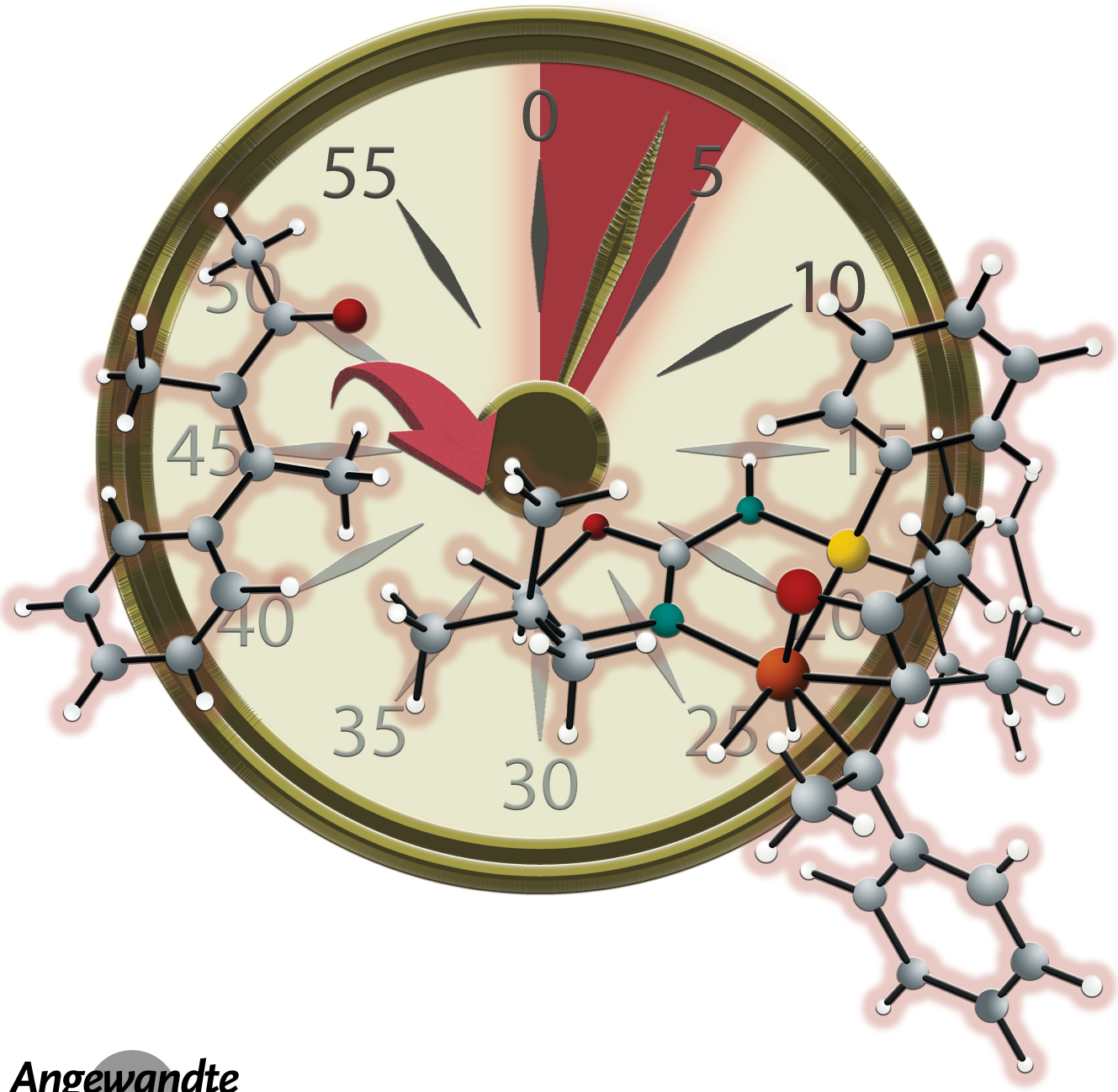

Abstract: Asymmetric hydrogenation (AH) of tetrasubstituted olefins generating two stereocenters is still an open topic. There are only a few reports on the AH of tetrasubstituted olefins with conjugated functional groups, while this process can create useful intermediates for the subsequent elaboration of relevant end products. Most of the tetrasubstituted olefins successfully submitted to AH belong to a small number of functional classes; remarkably, the AH of tetrasubstituted acyclic enones still represents an unsolved challenge. Herein, we disclose a class of air-stable Ir–P,N catalysts, prepared in three steps from commercially available amino alcohols, that can hydrogenate, in minutes, a wide range of electronically and sterically diverse acyclic tetrasubstituted enones (including exocyclic ones) with high yields and high enantioselectivities. The factors responsible for the excellent selectivities were elucidated by combining deuterogenation experiments and theoretical calculations. The calculations indicated that the reduction follows an Ir^{I}/Ir^{III} mechanism, in which enantioselectivity is controlled in the first migratory insertion of the hydride to the most electrophilic olefinic C_β and the formation of the hydrogenated product via reductive elimination takes place prior to the coordination of dihydrogen and the subsequent oxidative addition. The potential of the new catalytic systems is demonstrated by the derivatization of hydrogenation products.

Introduction

Nowadays, a large list of pharmaceutical formulations, agrochemicals and fine chemicals are manufactured using chiral chemicals. The global market for chiral chemicals was estimated at USD 58 billion in 2021 and is projected to reach USD 150 billion by 2030, illustrating increasing concerns on safety use, specificity and atom economy.[1] One of the most powerful methods for producing enantiomerically pure products is the catalytic asymmetric hydrogenation (AH) of olefins.[2] This process is 100 % atom economical and has been successfully used to produce single enantiomer intermediates, particularly in the pharmaceutical industry. The relevance of this process explains the continued interest of major pharmaceutical and fine chemical companies, such as AstraZeneca, Novartis, Merck, Johnson Matthey and Bayer, among others, on catalytic asymmetric hydrogenation.[3,4] The plethora of relevant results achieved in this field since the foundations of asymmetric catalysis may suggest that this is a rather saturated field. However, recent literature contradicts this viewpoint. A recent patent review by Glorius, Leker et al. highlighted the industrial relevance of AH[5] and concluded that AH is mature but has not yet reached its maximal economic relevance and will continue to generate valuable patents and innovations.

Advances in the synthesis of chiral molecules are made possible by the expansion of the range of substrates that can be successfully hydrogenated, thus opening paths for synthesizing a wider variety of chiral molecules in enantiopure form. Tetrasubstituted olefins whose hydrogenation can provide enantioenriched products with two contiguous stereocenters are among the most interesting substrates that are worth studying.[6] This motif is present in many privileged scaffolds such as the agrochemical methyl jasmonate and tofacitinib, a JAK inhibitor used in the treatment of ulcerative colitis (Figure 1).[7] However, tetrasubstituted olefins are some of the most elusive substrates in this process due to both, the challenge in differentiating the two prochiral faces, which hinders enantiocontrol, and their intrinsic reluctance to hydrogenation, resulting from steric limitations to metal coordination. Compared to the progress made in the AH of di- and trisubstituted olefins, the reduction of tetrasubstituted olefins generating two stereocenters remains an open topic.[6]

Furthermore, there are only a few reports on the hydrogenation of tetrasubstituted olefins with functional groups that can create useful intermediates for subsequent elaboration of relevant end products.[6] Till now, most of the studied substrates belong to a small number of functional classes. For example, unlike the more studied AH of tetrasubstituted olefins adjacent to acid and esters functionalities,[8] enones require an additional degree of chemoselectivity control to avoid carbonyl reduction,[9] and examples of their double-bond reduction are rare. This contrasts with the current advances in the reduction of trisubstituted olefins with an acyl moiety directly attached to

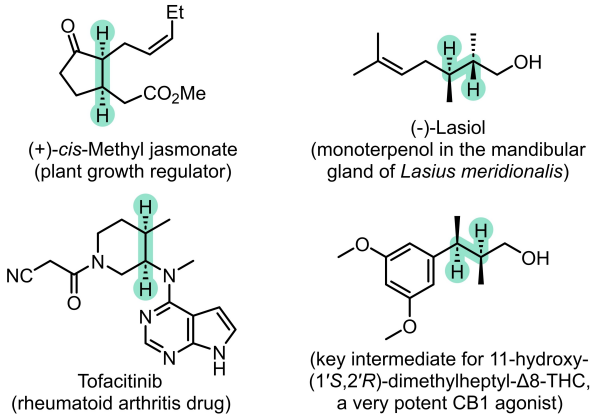

Figure 1. Examples of relevant bioactive and natural enantiopure compounds with two contiguous stereocenters.

[*] J. Faiges, Dr. M. Biosca, Prof. M. A. Pericàs, Dr. M. Besora, Prof. O. Pàmies, Prof. M. Diéguez
Universitat Rovira i Virgili, Departament de Química Física i Inorgànica
C/Marcel·lí Domingo, 1, 43007 Tarragona (Spain)
E-mail: maria.besora@urv.cat
montserrat.dieguez@urv.cat

an olefinic carbon (enones), where excellent enantioselectivities have been reported for a broad range of substrates using mainly Ir–P,N catalysts.[10] In addition, the tetrasubstituted substrates studied so far are mostly restricted to endocyclic olefins.[6] The added challenge with acyclic olefins is that double bond E/Z isomerization can occur under the experimental conditions required for hydrogenation. As a consequence of these multiple limitations, only three publications describe the AH of tetrasubstituted olefins of the enone class, always with a limited substrate scope.[8d,11] The Rh-Josiphos catalytic systems exhibits comparatively broader applicability, providing high diastereoselectivity and enantioselectivities in the range 77–96 %, although the use of an additive was required. In any case, enantioselectivities decreased to 67 % *ee* with acyclic substrates.[11b] More recently, Andersson's group reported a successful hydrogenation of one acyclic enone with an Ir-catalyst.[8d]

In the present situation, further work towards the mechanistic understanding of the process allowing improved predictability is still needed as a preliminary step to the identification of more general and selective catalysts for the AH of this type of substrates. In this article we report a new Ir–P,N catalyst which turns out to be the first generally applicable catalytic system for the highly enantio- and diastereoselective hydrogenation of α,β-unsaturated ketones involving an acyclic tetrasubstituted olefin component (including exocyclic ones). Thorough theoretical studies based on DFT calculations and deuterogenation experiments allowed the rationalization of the origin of enantioselectivity, the identification of the preferred reaction pathway, and the accurate prediction of enantioselectivities. We also show the potential uses of the resulting hydrogenated substrates by their further derivatization into useful compounds.

Results and Discussion

Catalyst Development and Optimization Studies

We began our study with the AH of the acyclic (*E*)-3-methyl-4-phenylpent-3-en-2-one (**1a**) as a representative substrate. We initially screened two sets of catalysts, with Rh and Ir respectively (see Supporting Information). The first set was based on previously known Rh-diphosphine catalysts (Rh/**L1**–**L6**, see Supporting Information) selected among the best candidates for the AH of functionalized olefins (including the previously mentioned Rh-Josiphos type catalysts, see Supporting Information).[2c,11b] The second set was a selection of Ir–P,N catalysts that had successfully hydrogenated trisubstituted α,β-unsaturated ketones (Ir/**L7**–**L10** and **L14**)[10a,d,e,i,n] and tetrasubstituted non-chelating cyclic and acylic olefins (Ir/**L11**–**L17**).[10i,n,12] The initially tested conditions were those reported to be optimal for other types of tetrasubstituted olefins, and depended on the employed metal (see Supporting Information for details). Among the results obtained with Rh-catalysts, the best catalytic performance was reached with the Rh-Josiphos systems, albeit with low conversion (up to 11 %) and a moderate enantioselectivity of 47 % *ee*, in line with the results reported with the Rh-Josiphos systems with lineal enones[11b] and the challenge that this type of substrates represents. On the other hand, all the Ir-catalysts resulted in very low conversions, the best being the one with ligand **L17** that forms a five-membered ring metal chelate, the smallest in the whole series (11 % conversion and 35 % *ee*). The reason for the somewhat better performance exhibited by this ligand could have its origin in the already mentioned, 5-membered nature of the chelate ring formed upon coordination to Ir, which allows the bulky tetrasubstituted olefins to be better accommodated. Next, we replaced the phosphine moiety in ligand **L17** by a *N*-phosphine group and prepared the corresponding Ir-catalyst precursor **I** (Scheme 1).[13] This new ligand boosted the activity, improved enantioselectivity (60 % *ee* in the (*S*,*S*)-**2a** product) and gave excellent diastereoselectivity (>25/1 dr) at room temperature under 100 bars of H_2 (see Table 1, entry 1).

The Ir-catalyst **I** containing the new chiral aminophosphine-oxazoline ligand is modular and the synthesis only requires three steps (Scheme 1). This facilitates the fine tuning of the ligand characteristics to optimize the catalytic behavior. We therefore tested catalysts precursors **I**–**VI** (Table 1), and the results showed that the nature of the oxazoline and the aminophosphine moieties affected significantly both activity and enantioselectivity. A bulky *tert*-butyl substituent at C-4 on the oxazoline skeleton (R^1) and aryl-based-aminophosphines (R^2 = aryl) were required to boost the activity and selectivity of the system (entries 1–6). Gratifyingly, the use of catalyst precursors **V** and **VI**, that possess the optimal ligand parameters, yielded the desired product (*S*,*S*)-**2a** in quantitative form with excellent diaster-

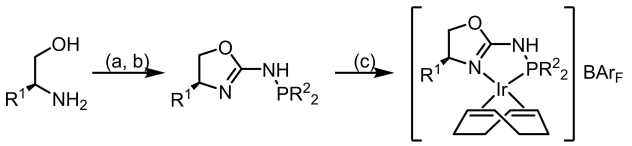

Scheme 1. Synthesis of novel Ir/aminophosphine-oxazoline catalyst precursors **I**–**VI**. (a) Br_2, NaCN, MeOH, 0 °C to rt, 2 h; (b) $ClPR^2_2$, NEt_3, THF, rt, 18 h; (c) $[Ir(\mu\text{-}Cl)(cod)]_2$, $NaBAr_F$, CH_2Cl_2, rt, 80 min (cod = 1,5-cyclooctadiene; BAr_F = tetrakis[3,5-bis(trifluoromethyl)phenyl]borate).

Table 1: Asymmetric hydrogenation of tetrasubstituted α,β-unsaturated enone **1a** using catalyst precursors **I**–**VI**.

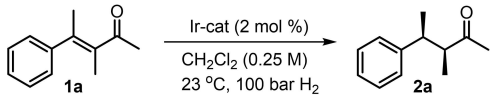

Entry	Ir-cat	%Conv (min)[a]	dr[a]	%ee[b]
1	**I**	76 (120)	>25/1	60 (*S*,*S*)
2	**II**	100 (120)	>25/1	92 (*S*,*S*)
3	**III**	100 (120)	>25/1	87 (*S*,*S*)
4	**IV**	49 (120)	>25/1	73 (*S*,*S*)
5	**V**	100 (5)	>25/1	>99 (*S*,*S*)
6	**VI**	100 (5)	>25/1	>99 (*S*,*S*)
7[c]	**V**	98 (360)	>25/1	>99 (*S*,*S*)
8[d]	**V**	100 (120)	>25/1	99 (*S*,*S*)
9[e]	**V**	100 (360)	10/1	>99 (*S*,*S*)

[a] Determined by GC. [b] Determined by GC using CP-Chirasil-Dex CB column. [c] Reaction carried out at using 0.5 mol% of **V**. [d] Reaction carried out at 50 bar H_2. [e] Reaction carried out at 1 bar H_2.

eo- and enantioselectivity (>25/1 dr and >99% *ee*) in only 5 minutes at room temperature.

Interestingly, the reaction could also be run at 0.5 mol% of catalyst loading and with reduced H_2 pressures (50 bars) maintaining the excellent enantioselectivity and diastereoselectivity (entries 7 and 8). Diastereoselectivity eroded, however, when the pressure was lowered to 1 bar of H_2 (entry 9). To explain the effect of the hydrogen pressure in the diastereoselectivity, we conducted deuterogenation experiments at 75 and 1 bar of D_2 (Scheme 2). At 75 bars, deuterium incorporation was only observed at the olefinic carbons, which agrees with a direct hydrogenation of the double bond. However, at 1 bar, deuteration at the methyl group of the α-position was also detected. This indicates that isomerization to the terminal olefin (*S*)-3-methylene-4-phenylpentan-2-one (**3**) (Scheme 2) takes place and its hydrogenation competes with the direct hydrogenation of **1a**, which explains the deleterious effect on diastereoselectivity observed at low hydrogen pressure.

Scope of the Reaction

We first examined the electronic effect of the aromatic ring in α,β-unsaturated ketones with *E*-geometry, bearing different electron-withdrawing and electron-donating groups at the *para*- and *meta*- positions (Table 2, substrates **1a**–**1h**). Both catalyst **V** and **VI** were highly successful, affording in only five minutes the desired chiral ketones **2a**–**2h** in high yields and stereoselectivities (dr's >25/1 and *ee*'s ranging from 96 to >99% (3*S*,4*S*); Table 2) except for ketone **2g**, whose diastereoselectivity was slightly lower (15/1) and the *para*-methyl substituted ketone **2h** for which diastereoselectivity was moderate (6.5/1). The hydrogenation of the corresponding *Z*-enones of **1a** and **1h** gave access to the (3*S*,4*R*) products **2i** and **2j** in high *ee*'s (up to 93%), albeit with somewhat lower diastereoselectivity (dr's up to 11/1). This suggests that the lower diastereocontrol seen in the hydrogenation of *para*-methyl substituted enone **1h** could arise from a competing *E*/*Z* isomerization process under hydrogenation conditions. To study the origin of the somewhat lower diastereoselectivity observed in the AH of *Z*-enones, we performed deuterogenation experiments with *Z*-enone **1j** (Scheme 3). We observed that deuterium was incorporated at the olefinic carbons as well as at the α-methyl substituent. This confirms that *Z*-enones are prone to isomerize to 1,1-disubstituted alkenes under the AH reaction conditions, which provides an explanation for the diastereoselectivities achieved in the AH of these *Z*-substrates.

A particular outcome found during the AH of the highly electron-rich enone **1f** was that the acyl group is also hydrogenated at prolonged reaction times (Scheme 4). Interestingly, the expected alcohol product was not observed and instead we observed the formation of 1,2,3-trimethyl-2,3-dihydro-1H-indene derivative **4**, with three stereogenic centers, as a mixture of 3 diastereoisomers at a ratio of 2.2/1.5/1 in almost enantiopure form (Scheme 4). The formation of the later arises from the fast protonation of the alcohol followed by C–O bond cleavage to form the corresponding carbocation, which undergoes intramolecular Friedel–Crafts alkylation to form the corresponding indane derivative **4** under the employed reaction conditions (see Supporting Information).[14,15]

Next, we extended the substrate scope even further. Interestingly, the catalyst also tolerates well the presence of other functional groups, such as pinacolborane, ester and

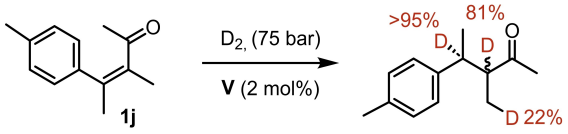

Scheme 3. Deuterogenation experiments of **1j** using catalyst precursor **V**. Percentages of deuterium incorporation shown in red.

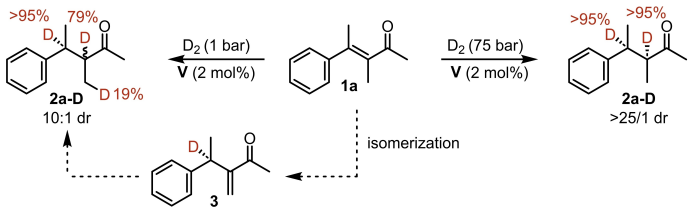

Scheme 2. Deuteration experiments of **1a** using catalyst precursor **V**. Percentages of deuterium incorporation shown in red.

Table 2: Substrate scope.[a]

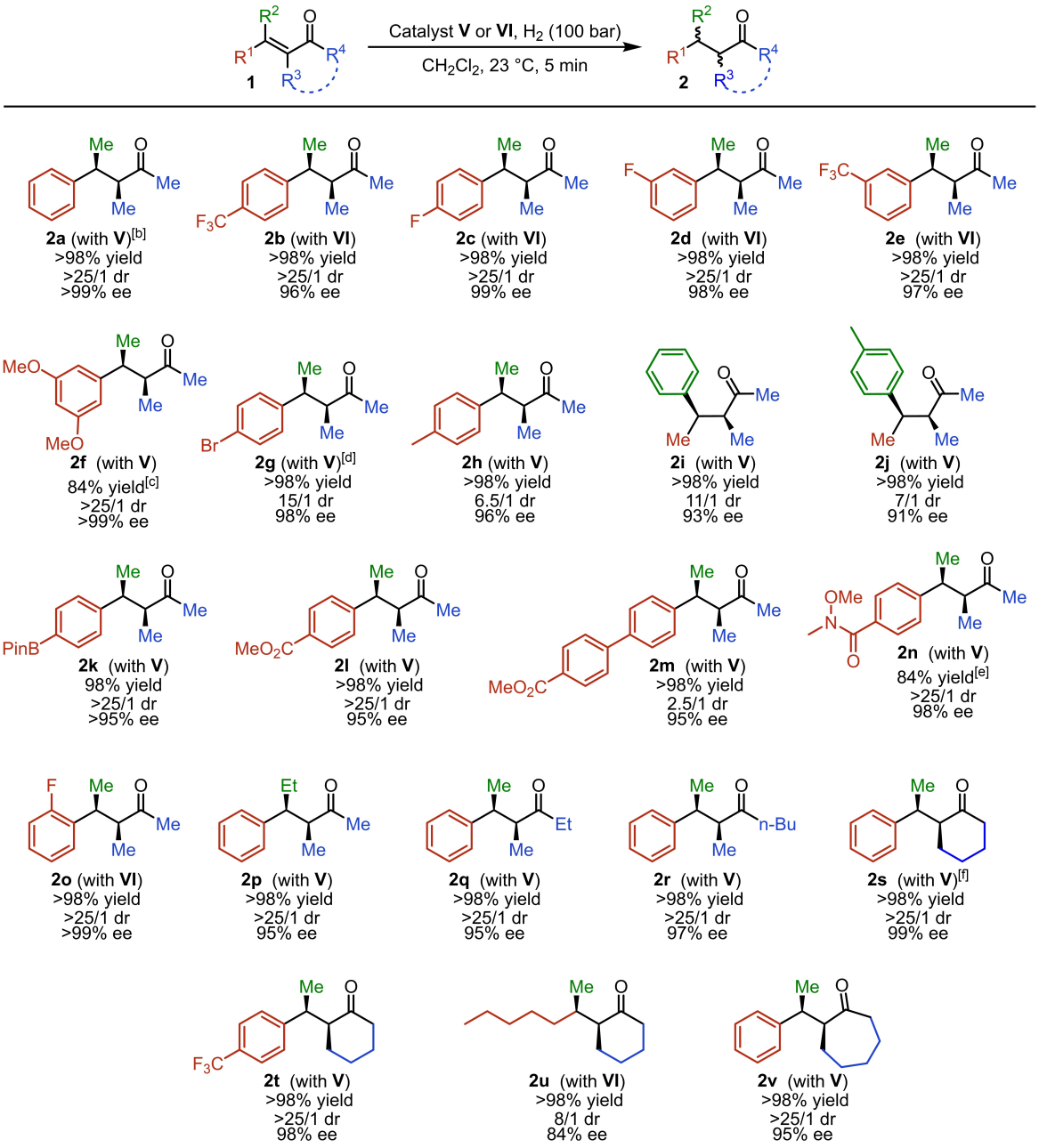

[a] Reaction conditions: **1** (0.25 mmol), Ir-complex (2 mol%), CH_2Cl_2 (2 mL). Absolute configuration determined upon derivatization of **2a** and **2i** to the corresponding 3-phenylbutan-2-yl acetates (see Supporting Information). [b] The reaction carried out at 6 mmol scale results in 1.04 g of **2a** (98.5% yield), >25/1 dr and 99% ee. [c] Reaction carried out for 3 min. [d] The reaction at 0.5 mol% catalyst loading results in 97% yield, 15/1 dr and 98% ee after 6 h. [e] Reaction carried out using 4 mol% of Ir-catalysts for 6 h. [f] The reaction at 0.5 mol% catalyst loading results in 94% yield, >25/1 dr and 99% ee after 6 h.

Weinreb amide (compounds **2k**–**2n**; dr's up to >25/1 and ee's up to 98%).

Excellent results were also obtained for the ortho fluorinated product **2o**, which was isolated in almost quantitative yield and with high diastereoselectivity (>25/1) and *ee* (>99%). The effect of the substituent at the β-position was studied with enone **1p**, bearing an ethyl group at that position. Again, saturated ketone **2p** was obtained in high yields, with very high diastereoselectivity (>25/1) and high enantioselectivity (95% *ee*). The effect of the enone substituent and of the substituent at the α-position were also investigated with substrates **2q**–**2v**, affording high yields and selectivities (typically >25/1 dr and ≥95% *ee*). Thus, enones bearing ethyl or n-butyl substituents at the ketonic carbonyl group were successfully hydrogenated to the desired ketones **2q** and **2r** with excellent diastereo- and enantiocontrol. The

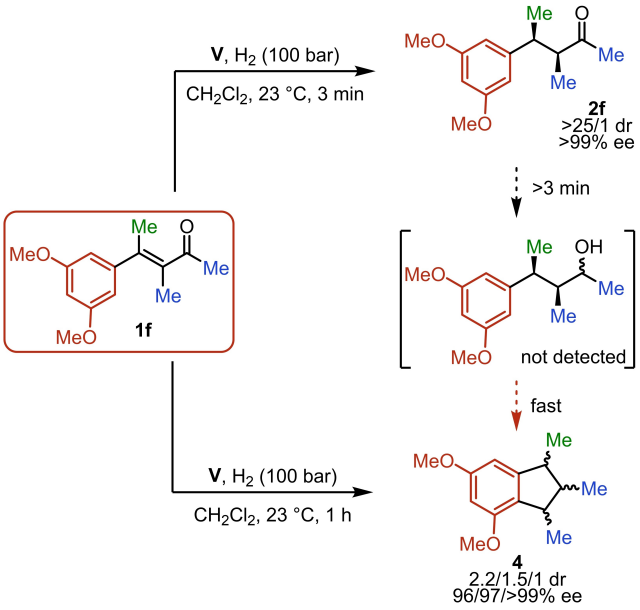

Scheme 4. Formation of chiral 1,2,3-trimethyl-2,3-dihydro-1H-indane derivative **4** under hydrogenation conditions at reaction times greater than 3 minutes.

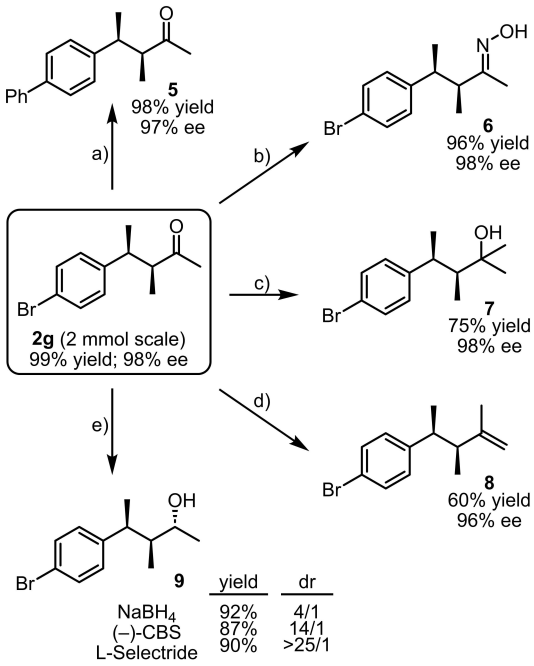

Scheme 5. Derivatization of the resulting enantioenriched hydrogenation products. Reaction conditions: a) $PhB(OH)_2$, $Pd(PPh_3)_4$, Cs_2CO_3, dioxane/H_2O (10:1), reflux; b) $NH_2OH{\cdot}HCl$, NaOAc, EtOH, 50 °C; c) MeMgBr, Et_2O, rt; d) $[Ph_3PMe]Br$, BuLi, THF, 40 °C and e) $NaBH_4$, MeOH, 0 °C to rt; or (−)-CBS, BH_3, THF, 0 °C; or L-Selectride, THF, −78 °C for 2 h then rt.

results in the preparation of **2r** (97 % *ee*) clearly surpass the 65 % *ee* reported for the only linear substrate tested with the Rh-Josiphos catalyst.[11b] The good results were also extensive to four rarely studied exocyclic tetrasubstituted olefins. These cyclic enones bearing an exocyclic double bond could be hydrogenated in similar excellent yields and high selectivities (chiral enones **1s**–**1v**). These are interesting results, since the AH of exocyclic olefins is more difficult than the AH of related endocyclic substrates and only a few examples have been reported, none of them involving a tetrasubstituted olefin.[16]

Potential Uses

To demonstrate the utility of the developed methodology, we initially carried out simple derivatizations of one of the enantiomerically pure ketones bearing two adjacent chiral centers at the α and β positions (**2g**; Scheme 5). We started with the Suzuki–Miyaura reaction, as one of the most popular cross coupling reactions, widely used in the total synthesis of natural products and drugs.[17] We were pleased to find that enantioenriched **2g** could undergo C–C coupling, leading to **5** with preservation of the stereochemical integrity. Similarly, **2g** was also subjected to oxime formation (**6**), Grignard reaction with methylmagnesium bromide leading to **7** and Wittig methylenation leading to **8**, in all cases without erosion in the enantiomeric purity of **2g**. These results widen the chemical space for the preparation of natural products or drugs analogues bearing two adjacent stereocenters.

Furthermore, we also focused on the formation of contiguous 1,2,3-*Me,Me,OH* stereotriads, which are present in many natural products and drug candidates, such as derivatives of lasiol[7b] and of 11-hydroxy-(1′*S*,2′*R*)-dimethylheptyl-Δ8-THC, a very potent CB1 agonist,[7c] whose stereoselective formation has not been previously achieved via straightforward asymmetric hydrogenation.[18] For this purpose, we studied the reduction of enantioenriched **2g** with $NaBH_4$, (−)-CBS and L-Selectride (Scheme 5). Positively, we found that the latter provided a completely selective reduction of the carbonyl group, leading to (2*R*,3*S*,4*S*)-**9** with complete diastereocontrol. The configuration of the new C–OH bond was established using CALB kinetic resolution of the diastereomeric mixture of **9** (see Supporting Information).

Mechanistic Insights

Several reaction mechanisms have been proposed for the AH of unfunctionalized olefins with Ir–P,N/C,N, for instance the Ir^{III}/Ir^{V} mechanisms by Andersson[19a,f] and by Burgess,[19b,d,e] supported by Pfaltz[19h] or the Ir^{I}/Ir^{III} mechanism with product coordination by Chen and Dietiker,[19c] supported by Buriak.[20] The presence of a carbonyl group in the substrate can have a significant impact on the mechanism of the reaction. Using an Ir-carbene,N system, Burgess et al. early found a reversed stereochemistry in the reduction of trisubstituted α,β-unsaturated esters in comparison to unfunctionalized olefins or allylic alcohols. Computational studies on these carbonyl-containing substrates supported the Ir^{III}/Ir^{V} mechanism with the coordination of the carbonyl

group to the metal center instead of the coordination of the hydrogen molecule found in the cycles proposed above.[19e] In contrast, Zhang studied by NMR and DFT the hydrogenation of exocyclic unsaturated carbonyl substrates with an Ir-BiphPHOX catalyst and proposed an Ir^{I}/Ir^{III} cycle where the substrate is exclusively coordinated through the olefin.[21] More recently, Bolm et al. investigated by computational methods the mechanism of the reduction of α,β-trisubstituted unsaturated enones with an Ir–P,N catalyst,[19i] identifying an Ir^{III} during the entire catalytic cycle and similar to that proposed by Burgess with the ketone forming a stable chelate.

On the basis of Bolm's study, we performed a computational study (B3LYP-D3/cc-pVTZ PCM|B3LYP-D3/6-31g-(d,p)+LANL2DZ PCM, see computational details in Supporting Information) of the AH process with our catalyst **V** and the tetrasubstituted olefin **1a** as the substrate. As starting point of the catalytic cycle, we computed the Ir-dihydride complexes with the enone coordinated in a bidentate fashion (see Supporting Information). In this calculation we considered all possible coordination patterns of the substrate and the most stable was $AM_{1Re/transP}$, with the enone coordinated through the *Re* face, and the acyl group in equatorial position and *trans* to the P atom, see Supporting Information. From this species there are two mechanistic possibilities (Scheme 6a); one of them involves migratory insertion (path A), while the other involves hydrogen addition following the Ir^{III}/Ir^{V} mechanism established by Andersson (path B). From these mechanistic possibilities, migratory insertion (path A) is energetically preferred; however, it has only a low energy barrier from isomers with the acyl group in axial position, as the process is favored when the hydride is in the same plane of the olefin. Among those isomers, the most stable is $AM_{2Re/transN}$. In any case, the other axial isomers are quite close in energy and cannot be disregarded. We therefore computed all possible transition states (TSs) for the migratory insertion from all possible dihydride isomers with the acyl group coordinated in axial position, considering also that the migratory insertion can take place at either the α or the β olefinic carbons (for a detailed discussion see Supporting Information). The results indicated that the migratory insertion to the more electrophilic β carbon is favored, which is in line with Bolm's findings and differs from the Burgess proposal. The most stable transition state is $ATS_{1Re/β/transN,}$ located at 10.9 kcal.mol^{-1} above $AM_{1Re/transP}$, and closely followed by $ATS_{1Re/β/transP}$ and $ATS_{1Si/β/transN}$ at 0.1 and 1.4 kcal.mol^{-1} above, respectively. After this insertion, intermediate AM_3 with the acyl group in axial position is formed (Scheme 6). AM_3 can undergo hydrogen coordination (path A) but also can easily undergo isomerization to form a most stable intermediate CM_3 with the acyl group in equatorial position (path C). We found that although CM_3 can then undergo hydrogen coordination, the concomitant σ-bond metathesis CTS_3 to form the final product is not energetically feasible, and path C can also be discarded (see details in Supporting Information). So, path A would continue via dihydrogen coordination in AM_3, σ-bond metathesis of the dihydrogen and formation of the hydrogenated product with the generation of Ir^{III} species (Scheme 6a, see Supporting Information for details). The highest energetic barrier is associated to dihydrogen coordination, ATS_2 is located at 15.2 kcal.mol^{-1} (Scheme 6a). Even if this mechanism is energetically plausible, the fact that the hydrogen coordination is the most energetically demanding step contrasts with the mechanism proposed by Bolm and co-workers and fails to provide a reasonable explanation for the observed very high enantiomeric control.

We therefore further explored the potential energy surface looking for other mechanistic possibilities. As a result of this endeavor, we found a plausible Ir^{I}/Ir^{III} mechanistic pathway involving a reductive elimination prior to coordination of the hydrogen molecule, which we have termed path D (Scheme 6). Thus, the reductive elimination from CM_3 through DTS_2 followed by hydrogen coordination is easier than ATS_2. No transition state could be located for the hydrogen coordination and scans on the potential energy surface suggest the process is barrier less, hence the process is expected to be controlled by diffusion. At high pressures the diffusion rate will be faster than at low pressures and this can explain the differences in the *dr* found at different pressures. After coordination of a hydrogen molecule, a very exergonic oxidative addition of the dihydrogen leads to the final product. As can be seen in the Gibbs free energy profile presented in Scheme 6b, migratory insertion through ATS_1, is the rate and enantio-determining step. It is interesting to note that hydrogen coordination to DM_5 could become the rate determining step at conditions of low hydrogen pressures (low concentration), as it is close in energy to ATS_1 and has associated a diffusion barrier (see Supporting Information for more details and effect on *dr*). This Ir^{I}/Ir^{III} mechanism is the most energetically viable, with an exceptionally low barrier of 10.9 kcal.mol^{-1} for the rate limiting step. Moreover, it is the only one that explains the observed enantioselectivity through the analysis of the most endergonic transition states (ATS_1). Thus, the computed transition states ATS_1 predict well the enantioselectivity observed experimentally for **2a** as well as a for a range of other substrates (see calculations for **1b**, **1h**, **1i**, **1p**, **1q** and **1s** with catalyst **V** and also for **1a** with catalyst **VI**, see Supporting Information), which further demonstrates the robustness of the calculations. A very good agreement between experimental and computational *ee* was found with errors below 9 *ee* units, supporting the postulated mechanism calculations. These results support that this catalytic system follows a different mechanism from the ones previously proposed, although it must be mentioned that it resembles the mechanism proposed by Chen's, but with higher coordination number through the whole cycle due to keto group coordination. Another difference lies on the fact that in our proposal hydrogen coordination is predicted to take place prior to product release.[20c] Thus, in contrast to Bolm's finding, the formation of the hydrogenated product via reductive elimination takes place prior to the coordination of the dihydrogen and the subsequent oxidative addition. All presented mechanisms are discussed in more detail at the Supporting Information.

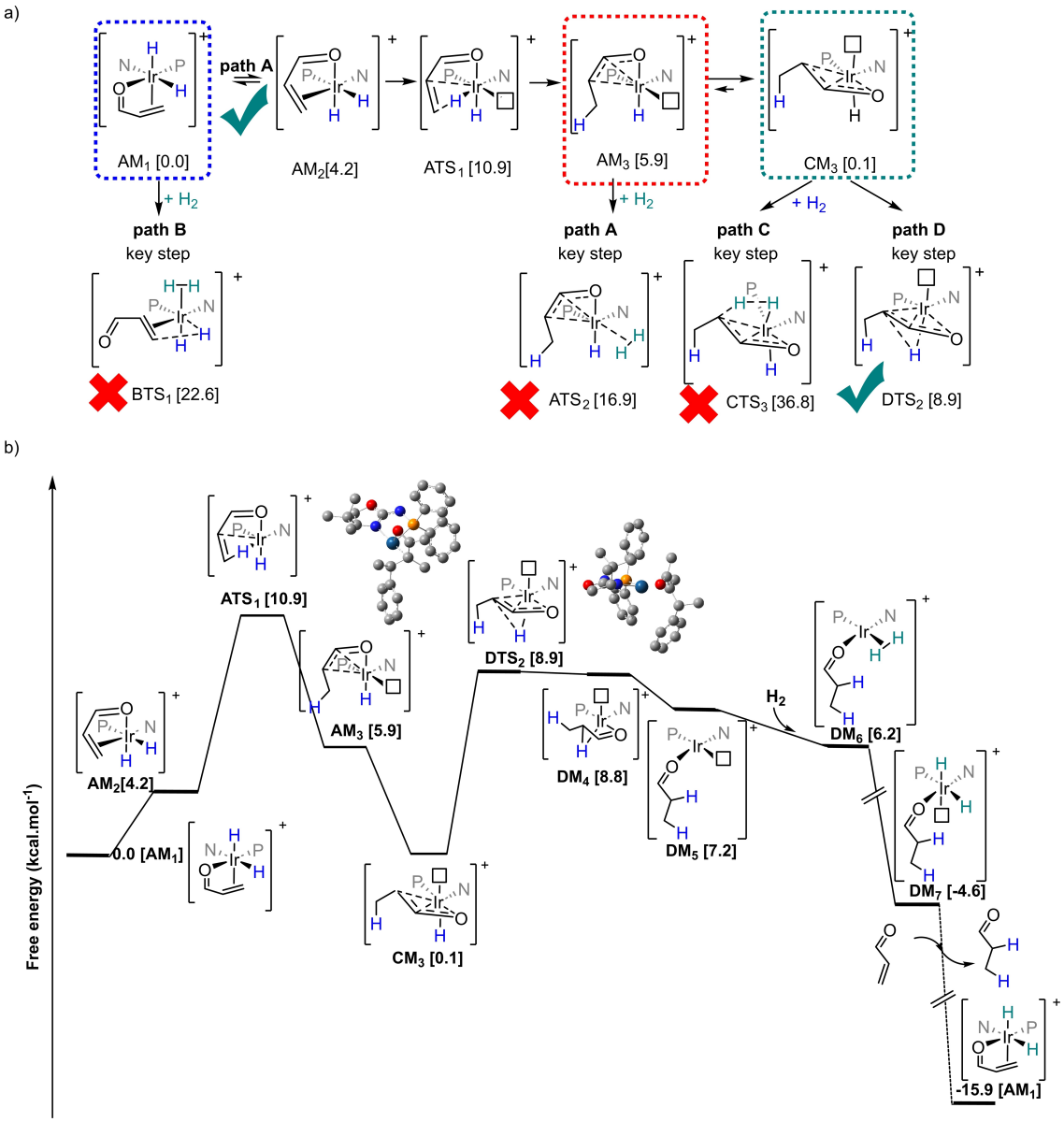

Scheme 6. a) Simplified Scheme of the mechanism studied for the AH of tetrasubstituted enone **1a** with catalyst **V**. Ligand abbreviated as P,N and substituents at the enone omitted for clarity. Energies correspond to Gibbs free energies in solution and in kcal.mol^{-1}. b) Free energy profile for the lowest energy mechanism (path D) for the catalytic hydrogenation of substrate **1a** mediated by catalyst **V**. In schematic representations the ligand has been simplified as P, N and in ball and stick geometries hydrogens have been omitted for clarity. Energies correspond to Gibbs free energies in solution and in kcal.mol^{-1}.

Analysis of the key TSs' structures

According to mechanism D (Scheme 6), the enantioselectivity of the process is determined at ATS_1. To uncover the factors responsible for the enantioselectivity we analyzed all stereoisomers of ATS_1 that contribute to the enantioselectivity. In this analysis both electronic and steric factors are important. All possible stereoisomers were carefully considered (olefin coordinated *trans* to the P or to the N atoms and through the *Re* or *Si* faces, and the insertion of the hydride at olefinic C_α or C_β, see Supporting Information for details). Electronic factors made migratory insertion to the more electrophilic C_β favored over the C_α. Moreover, stereoisomers that do not allow coordination of the ketone were destabilized, according to calculations. These two factors were very important to determine the enantioselectivity as they limit the number of low energy TSs to 4 (see Supporting Information for further details). The lowest energy TSs were two pro-*Re* species that differed in the olefin coordinated *trans* to the N or P and were separated by just 0.1 kcal.mol^{-1}, namely $ATS_{1Re/\beta/transN}$ and $ATS_{1Re/\beta/transP}$. These were followed by two pro-*Si* TSs: $ATS_{1Si/\beta/transN}$ at 1.4 kcal.mol^{-1} and $ATS_{Si/\beta/transP}$ at 6.2 kcal.mol^{-1}, with the olefin coordinated *trans* to the N and to the P, respectively. Steric factors of these four TSs were analyzed via quantitative quadrant-diagram representation using the MolQuO

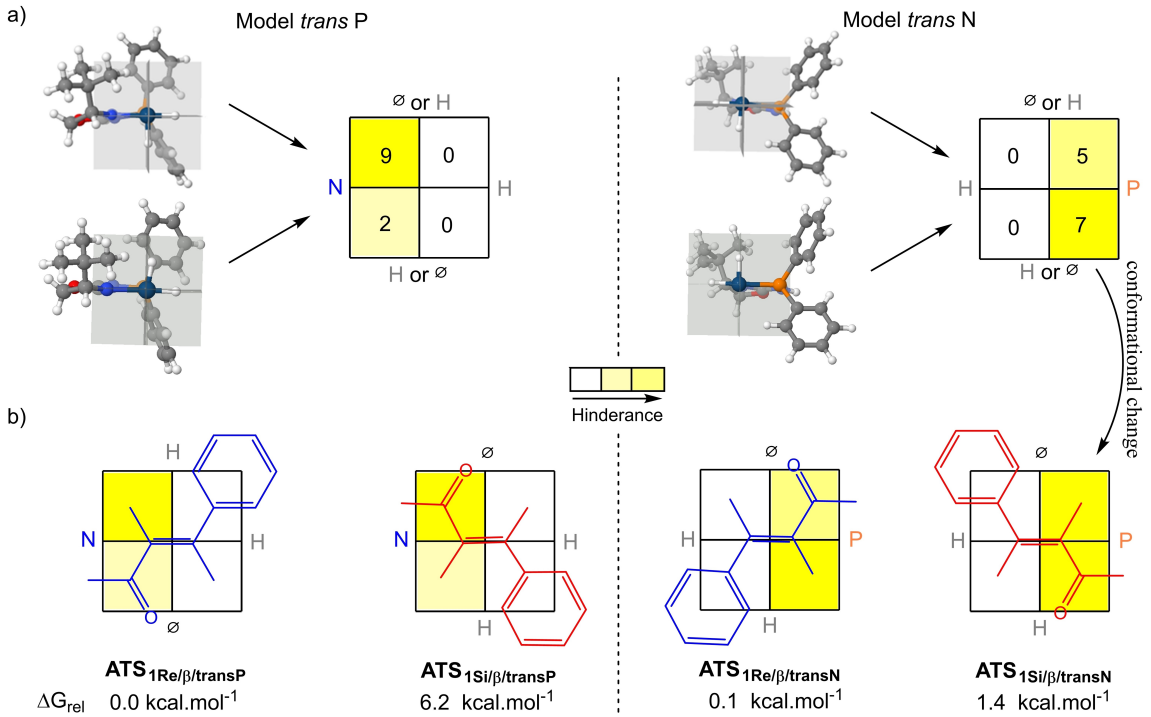

Figure 2. Quantitative quadrant diagram representation for catalyst **V** of both models (model *trans* P -left- and model *trans* N -right–) for a) Ir-catalysts without the olefin coordinated and b) most stable calculated transition states for substrate **1a**. The partial occupation of each quadrant according to MolQuO are shown.

software (Figure 2).[22] To begin with, we studied the system without the olefin, to analyze the disposition of the catalyst (Figure 2a). Considering that we had two models, either with the olefin coordinated *trans* to the P or *trans* to the N (Figure 2), the most occupied quadrant for the low-energy *trans* to the P stereoisomers is the upper left quadrant, where the oxazoline's group is located (see Figure 2a left). In contrast, for the stereoisomer *trans* to N, the lower right quadrant is the most occupied one, where the N-phosphine substituents are located (see Figure 2a right). In addition, the most reactive hydride is in equatorial position (*trans* to the N, for the model *trans* to P, and *trans* to P for the second model, see Figure 2a).

The expected behavior is that the olefin will coordinate preferentially with the least bulky substituent in the most occupied quadrant and the bulkiest substituent in the least occupied quadrant. The corresponding TS stabilities are expected to follow the same trend. However, the disposition of the olefin in this quadrant analysis is also controlled by the fact that *ee* is determined in the first migratory insertion of the hydride, which take place at the olefinic C_β. Therefore, the disposition of this carbon C_β, and consequently its substituents, in the quadrant will be controlled by the disposition of the most reactive hydride, which is in the equatorial position. In accordance, the four TSs presents the β olefinic substituents on the least hindered quadrants, the ones near to the equatorial hydride (see Figure 2b).

Both models also support the preferred coordination of the olefin through the *Re*-face, which leads to the formation of the major experimentally observed (3*S*,4*S*)-product. Accordingly, both pro-*Re* TSs present the best arrangement, because the most hindered area is occupied with the α olefinic methyl group, and the bulkier acyl group is in a less hindered area. In contrast, for the less favored pro-*Si* TSs the acyl group is located at the most hindered quadrant and the less bulky methyl group at the partially occupied quadrant, resulting in less favorable TSs. Interestingly, $ATS_{1Si/\beta/transN}$ is more stable than $ATS_{1Si/\beta/transP}$. This is because $ATS_{1Si/\beta/transN}$ can accommodate the olefin better since it reduces more the steric clash with the acyl group through rotation of the phenyl rings (of the phosphine), thus moving some of the steric hindrance to the upper quadrant where the less hindered methyl group is located (see more details and non-covalent interaction (NCI) plots in the Supporting Information).

According to this model one would expect little effect of the substituents in β-position of the substrate since these will be in the unoccupied quadrants. This explains the high enantioselectivities obtained with substrates **2a** to **2p** with a variety of substituents and the *E*/*Z*-isomers. In addition, the model also explains the good enantioselectivities obtained with substrates **2q** to **2v** because the substituent of the ketone destabilizes the TSs of the *Si*-face, thus increasing the energy gap between the pro-*Re* and the pro-*Si* TSs.

Conclusion

In this study we developed a new family of Ir–P,N catalysts for the asymmetric hydrogenation of elusive tetrasubstituted

acyclic enones. These catalysts have interesting capabilities: they are air-stable and fast (full conversion in minutes), lead to high yields (>98%) and high stereoselectivity (up to >25/1 dr and 99% ee) and have quite a broad and interesting substrate scope, including some precursors of natural products and potential drugs, in addition to being prepared in only 3 steps.

Deuterogenation experiments and theoretical calculations have been used to explore the reaction mechanism and have reproduced the experimental observations. The mechanism differs from the ones previously proposed with Ir-catalysts used in the AH of trisubstituted olefins conjugated with carbonyl groups. According to our calculations, the preferred mechanism is an Ir^{I}/Ir^{III} pathway with a very low overall barrier of just 10.9 kcal.mol^{-1}. This barrier corresponds to the first migratory insertion of the hydride to the most electrophilic olefinic C_{β}, which is in line with Bolm's finding but differs from Burgess proposal. Afterwards and in contrast with Bolm's finding, the formation of the hydrogenated product via reductive elimination takes place prior to the coordination of the dihydrogen. The transition states responsible for enantioselectivity have been analyzed and two main factors contribute to the high enantioselectivity: i) the number of low energy transition states is reduced thanks to bidentate substrate coordination and the need of a hydride at the olefin plane for the migratory insertion to take place; and ii) the ^{t}Bu group of catalysts **V** and **VI** and the phosphine substituents maximize enantioselectivity.

Supporting Information

Preliminary catalyst screening, synthesis of catalysts and substrates, post-modifications, characterization details and enantiomeric excess determination of hydrogenated products, copies of NMR spectra and GC or HPLC traces for *ee* determination of hydrogenated products, computational details, detailed discussion on the mechanism and origin of the enantioselectivity, calculated energies and computed cartesian coordinates for all TSs and deuterogenation experiments (PDF).

Acknowledgements

This work was supported by grants from FEDER/Ministerio de Ciencia e Innovación (MICINN)/AEI (PID2019-104904GB-I00, PID2022-139996NB-I00, PID2021-128128NB-I00 and CNS2022-136079). Grants 2021SGR00163 and 2021SGR00110 funded by the Catalan Government are also gratefully acknowledged. J. F. also thanks Ministerio de Ciencia, Innovación y Universidades for FPU18/06352 fellowship. M. B. also thanks Ministerio de Ciencia e Innovación for a Juan de la Cierva fellowship.

Conflict of Interest

The authors declare no conflict of interest.

Data Availability Statement

The data that support the findings of this study are available in the supplementary material of this article.

Keywords: Asymmetric Hydrogenation · Iridium · Mechanism · N-Phosphine-Oxazoline · Tetrasubstituted Enones

[1] Chiral Chemicals Market report, https://www.nextmsc.com/report/chiral-chemicals-market.

[2] a) R. Noyori, *Asymmetric Catalysis in Organic Synthesis*, Wiley, New York, **1994**; b) *Comprehensive Asymmetric Catalysis* (Eds.: E. N. Jacobsen, A. Pfaltz, H. Yamamoto), Springer-Verlag, Berlin, **1999**; c) W. Tang, X. Zhang, *Chem. Rev.* **2003**, *103*, 3029; d) J.-H. Xie, S.-F. Zhu, Q.-L. Zhou, *Chem. Rev.* **2011**, *111*, 1713; e) Y. Zhu, K. Burgess, *Acc. Chem. Res.* **2012**, *45*, 1623; f) P. Etayo, A. Vidal-Ferran, *Chem. Soc. Rev.* **2013**, *42*, 728; g) J. J. Verendel, O. Pàmies, M. Diéguez, P. G. Andersson, *Chem. Rev.* **2014**, *114*, 2130; h) Z. Zhang, N. Butt, W. Zhang, *Chem. Rev.* **2016**, *116*, 14769; i) C. Margarita, P. G. Andersson, *J. Am. Chem. Soc.* **2017**, *139*, 1346; j) A. N. Kim, B. M. Stoltz, *ACS Catal.* **2020**, *10*, 13834; k) *Metal-catalyzed Asymmetric Hydrogenation. Evolution and Prospect in Advances in Catalysis, Vol. 68* (Eds.: M. Diéguez, A. Pizzano), Elsevier, Oxford, **2021**; l) A. Cabré, X. Verdaguer, A. Riera, *Chem. Rev.* **2022**, *122*, 269; m) *Catalytic Asymmetric Synthesis*, 4th ed. (Eds.: T. Akiyama, I. Ojima), John Wiley & Sons, Inc, Hoboken, **2022**.

[3] For a recent review, see: M. Biosca, M. Diéguez, A. Zanotti-Gerosa, Asymmetric hydrogenation in Industry. *Adv. Catal.* **2021**, *68*, 341 and references therein.

[4] For recent publications not included in reference [3], see: a) C. Schotes, S. Müller, *ACS Sustainable Chem. Eng.* **2022**, *10*, 13244; b) S. Feng, H. Zhang, Z. Tang, X. Peng, M. Yang, X. Wei, W. Zhong, *Org. Process Res. Dev.* **2022**, *26*, 3089; c) J. M. Kallemeyn, J. Hartung, T. Connolly, A. Ickes, B. Kotecki, L. Van Haandel, M. Nazari, O. Manjrekar, S. Chen, *Org. Process Res. Dev.* **2022**, *26*, 2947; d) S. N. Greszler, G. Zhao, B. Shelat, E. A. Voight, *Org. Lett.* **2022**, *24*, 7305; e) M. J. Rozema, L. Bhagavatula, A. Christesen, T. B. Dunn, A. Ickes, B. J. Kotecki, J. C. Marek, E. Moschetta, W. H. Morrill, M. Mulhern, M. Rasmussen, T. Reynolds, S. Yu, *Org. Process Res. Dev.* **2022**, *26*, 949; f) S. Feng, B. Ren, L. Li, F Xia, Z. Tang, Y. Zhang, X. Liu, Q. Luc, W. Zhonga, *Org. Chem. Front.* **2022**, *9*, 3022; g) R. T. Ruck, N. A. Strotman, S. W. Krska, *ACS Catal.* **2023**, *13*, 475; h) R. Frutos, T. G. Tampone, J. Mulder, J. Gao, J. D. Sieber, S. Rodriguez, N. Haddad, K. Baer, J. Brown, B.-S. Yang, R. Giovannini, J. J. Song, N. Grinberg, H. Lee, C. H. Senanayake, *Org. Process Res. Dev.* **2023**, *27*, 505.

[5] M. A. Stoffels, F. J. R. Klauck, T. Hamadi, F. Glorius, J. Leker, *Adv. Synth. Catal.* **2020**, *362*, 1258.

[6] S. Draft, K. Ryan, R. B. Kargbo, *J. Am. Chem. Soc.* **2017**, *139*, 11630.

[7] See for instance: a) G. Sembder, B. Parthier, *Annu. Rev. Plant Physiol. Plant Mol. Biol.* **1993**, *44*, 569) ((−)-*cis* methyl jasmonate; b) T. Kasai, H. Watanabe, K. Mon, *Bioorg. Med. Chem.* **1993**, *1*, 61 ((+)-lasiol); c) J. Liddle, J. W. Huffman, *Tetrahedron* **2001**, *57*, 7607; d) J. M. Kremer, B. J. Bloom, F. C. Breedveld, J. H. Coombs, M. P. Fletcher, D. Gruben, S. Krishnaswami, R. N. Burgos-Vargas, B. Wilkinson, C. A. F. Zerbini, S. H. Zwillich, *Arthritis Rheum.* **2009**, *60*, 1895; e) E. Martínez-Lopez, A. J. García-Dernánadez. in *Encyclopedia of Toxicology*, 3rd ed. (Ed.: P. Wexler), Elsevier, Amsterdam, **2014**, p 586; f) A. Gradman, R. Schmieder, R Lins, J.

Nussberger, Y. Chiang, M. Bedigian, *Circulation* **2005**, *111*, 1012; g) M. C. Desai, S. L. Lefkowitz, P. F. Thadeio, K. P. Longo, R. M. Snider, *J. Med. Chem.* **1992**, *35*, 4911; h) G. R. Sareddy, X. Li, J. Liu, S. Viswanadhapalli, L. Garcia, A. Gruslova, D. Cavazos, M. Garcia, A. M. Strom, J. A. Gustafsson, R. R. Tekmal, A. Brenner, R. K. Vadlamudi, *Sci. Rep.* **2016**, *6*, 24185.

[8] a) S. Song, S. F. Zhu, Y. Li, Q. L. Zhou, *Org. Lett.* **2013**, *15*, 3722; b) S. F. Zhu, Q. L. Zhou, *Acc. Chem. Res.* **2017**, *50*, 988; c) S. Ponra, W. Rabten, J. Yang, H. Wu, S. Kerdphon, P. G. Andersson, *J. Am. Chem. Soc.* **2018**, *140*, 13878; d) S. Kerdphon, S. Ponra, J. Yang, H. Wu, L. Eriksson, P. G. Andersson, *ACS Catal.* **2019**, *9*, 6169; e) M. Biosca, E. Salomó, P. de la Cruz-Sánchez, A. Riera, X. Verdaguer, O. Pàmies, M. Diéguez, *Org. Lett.* **2019**, *21*, 807; f) Q.-K. Zhao, X. Wu, L.-P. Li, F. Yang, J.-H. Xie, Q.-L. Zhou, *Org. Lett.* **2021**, *23*, 1675.

[9] Zhou and co-workers recently used chiral spiro-iridium catalysts for the reduction of tetrasubstituted cyclic α-carboxylated enones to chiral cycloalkanols. However, the carbonyl group was also reduced. See: Y.-T. Liu, J.-Q. Chen, L.-P. Li, X.-Y. Shao, J.-H. Xie, Q.-L. Zhou, *Org. Lett.* **2017**, *19*, 3231.

[10] a) S. M. Lu, C. Bolm, *Angew. Chem. Int. Ed.* **2008**, *47*, 8920; b) W.-J. Lu, Y.-W. Chen, X.-L. Hou, *Angew. Chem. Int. Ed.* **2008**, *47*, 10133; c) F. Tian, D. Yao, Y. Liu, F. Xie, *Adv. Synth. Catal.* **2010**, *352*, 1841; d) J. Mazuela, P.-O. Norrby, P. G. Andersson, O. Pàmies, M. Diéguez, *J. Am. Chem. Soc.* **2011**, *133*, 13634; e) D. A. Woodmansee, M.-A. Müller, L. Tröndlin, E. Hörmann, A. Pfaltz, *Chem. Eur. J.* **2012**, *18*, 13780; f) J.-Q. Li, X. Quan, P. G. Andersson, *Chem. Eur. J.* **2012**, *18*, 10609; g) X. Liu, Z. Han, Z. Wang, K. Ding, *Angew. Chem. Int. Ed.* **2014**, *53*, 1978; h) J. Xia, Y. Nie, G. Yang, Y. Liu, I. D. Gridnev, W. Zhang, *Chin. J. Chem.* **2018**, *36*, 612; i) M. Biosca, M. Magre, O. Pàmies, M. Diéguez, *ACS Catal.* **2018**, *8*, 10316; j) M. Biosca, O. Pàmies, M. Diéguez, *J. Org. Chem.* **2019**, *84*, 8259; k) S. Ponra, J. Yang, S. Kerdphon, P. G. Andersson, *Angew. Chem. Int. Ed.* **2019**, *58*, 9282; l) B. B. C. Peters, J. Jongcharoenkamol, S. Krajangsri, P. G. Andersson, *Org. Lett.* **2021**, *23*, 242; m) B. B. C. Peters, J. Zheng, N. Birke, T. Singh, P. G. Andersson, *Nat. Commun.* **2022**, *13*, 361; n) M. Biosca, P. de la Cruz-Sánchez, J. Faiges, J. Margalef, E. Salomó, A. Riera, X. Verdaguer, J. Ferré, F. Maseras, M. Besora, O. Pàmies, M. Diéguez, *ACS Catal.* **2023**, *13*, 3020.

[11] a) V. Rautenstrauch, J.-J. Riedhauser, *World Patent WO00206*, **1996** (with only two examples of AH of cyclic tetrasubstituted ketones with ee's up to 90 % and a dr of 96/4); b) J. R. Calvin, M. O. Frederick, D. L. T. Laird, J. R. Remacle, S. A. May, *Org. Lett.* **2012**, *14*, 1038 (with 10 examples of cyclic olefins with *ee*'s in the range 77–96 % and one example of *E*- and *Z*- acyclic substrate with *ee*'s up to 67 %).

[12] a) M. G. Schrems, E. Neumann, A. Pfaltz, *Angew. Chem. Int. Ed.* **2007**, *46*, 8274; b) R. Bigler, K. A. Mack, J. Shen, P. Tosatti, C. Han, S. Bachmann, H. Zhang, M. Scalone, A. Pfaltz, S. E. Denmark, S. Hildbrand, F. Gosselin, *Angew. Chem. Int. Ed.* **2020**, *59*, 2844.

[13] Our group has recently shown the advantageous of a *N*-phosphine group into the ligand, see: ref. 10i vs ref. 10n.

[14] J.-Q. Li, J. Liu, S. Krajangsri, N. Chumnanvej, T. Singh, P. G. Andersson, *ACS Catal.* **2016**, *6*, 8342.

[15] Note that small traces of 1,2,3-trimethyl-1H indene were detected by GC/MS, which are arising from the cyclization of the corresponding formed allylic alcohol derivative. For more mechanistic insights see Supporting Information.

[16] The main challenge with exocyclic olefins is that the stereochemical outcome is highly influenced by ring size and, until recently, only a few examples had been able to provide high enantiocontrol for exocyclic olefins with different ring sizes for trisubstituted olefins. For successful examples, see: a) ref. 10g; b) M. Biosca, P. de la Cruz-Sánchez, D. Tarr, P. Llanes, E. A. Karlsson, J. Margalef, O. Pàmies, M. A. Pericàs, M. Diéguez, *Adv. Synth. Catal.* **2023**, *365*, 167; c) ref. 10n; For a recent study on the successful AH of exocyclic trisubstituted α,β,–unsaturated lactams, see: d) R. Zhang, S. Xu, Z. Luo, Y. Liu, J. Zhang, *Angew. Chem. Int. Ed.* **2023**, *62*, e202213600.

[17] See for instance: a) M. M. Heravi, E. Hashemi, *Tetrahedron* **2012**, *68*, 9145; b) R. Martin, S. L. Buchwald, *Acc. Chem. Res.* **2008**, *41*, 1461; c) I. P. Beletskaya, F. Alonso, V. Tyurin, *Coord. Chem. Rev.* **2019**, *385*, 137.

[18] Several polyketide, 1,3-hydroxymethyl, 1,2-dimethyl, 1,2-hydroxymethyl and 1,2,3-*Me,OH,Me* chirons have been attained via asymmetric hydrogenation of chiral allylic and homoallylic alcohols, see: ref. 2e.

[19] a) P. Brandt, C. Hedberg, P. G. Andersson, *Chem. Eur. J.* **2003**, *9*, 339; b) Y. Fan, X. Cui, K. Burgess, M. B. Hall, *J. Am. Chem. Soc.* **2004**, *126*, 16688; c) R. Dietiker, P. Chen, *Angew. Chem. Int. Ed.* **2004**, *43*, 5513; d) X. Cui, Y. Fan, M. B. Hall, K. Burgess, *Chem. Eur. J.* **2005**, *11*, 6859; e) J. Zhou, J. W. Ogle, Y. Fan, V. Banphavichit, Y. Zhu, K. Burgess, *Chem. Eur. J.* **2007**, *13*, 7162; f) T. L. Church, T. Rasmussen, P. G. Andersson, *Organometallics* **2010**, *29*, 6769; g) K. H. Hopmann, A. Bayer, *Organometallics* **2011**, *30*, 2483; h) S. Gruber, A. Pfaltz, *Angew. Chem. Int. Ed.* **2014**, *53*, 1896; i) J. Engel, S. Mersmann, P.-O. Norrby, C. Bolm, *ChemCatChem* **2016**, *8*, 3099; j) G. Helmchen, *Chem. Eur. J.* **2023**, *29*, e202301488.

[20] L. D. Vazquez-Serrano, B. T. Owens, J. M. Buriak, *Inorg. Chim. Acta* **2006**, *359*, 2786.

[21] Y. Liu, I. D. Gridnev, W. Zhang, *Angew. Chem. Int. Ed.* **2014**, *53*, 1901.

[22] a) S. Aguado-Ullate, S. Saureu, L. Guasch, J. J. Carbó, *Chem. Eur. J.* **2012**, *18*, 995; b) S. AguadoUllate, M. Urbano-Cuadrado, I. Villalba, E. Pires, J. I. García, C. Bo, J. J. Carbó, *Chem. Eur. J.* **2012**, *18*, 14026.

Manuscript received: October 20, 2023
Accepted manuscript online: December 13, 2023
Version of record online: December 28, 2023